In Vitro Mucin-Producing Models to Study Cystic Fibrosis

By
Matt Washko

Senior Honors Thesis
Biology
University of North Carolina at Chapel Hill

4/27/20

Approved:

_____

Amy Maddox, Thesis Advisor

Alaina Garland, Reader

Mehmet Kesimer, Reader

***In Vitro* Mucin-Producing Models to Study Cystic Fibrosis**

Matt Washko, Cameron Morrison, Lolita Radet, Camille Ehre

Abstract

Cystic Fibrosis (CF) is a genetic disease featuring a mutation in the CFTR gene that leads to a buildup of thick clumps of high-molecular-weight glycoproteins (mucins/MUCs) in the lungs and the intestines. This causes difficulty breathing, frequent infections, poor growth, nutrient malabsorption, and ultimately death. Although pulmonary complications are the most life threatening and the most studied, investigating intestinal physiology may provide better insight into the altered mucus properties and systemic effects of CFTR dysfunction. Our goal was to establish a model system to study the effects of CFTR function on gut mucus and to further characterize mucus properties in the intestine. The HT29 cell line, derived from a colon adenocarcinoma, was used in this project as it has previously proven to express both CFTR and mucin genes. To determine the most appropriate culture conditions and optimize expression of mucins and CFTR, HT29 cells were grown in different media, and the validity of the model was evaluated through resistance measurements, mucin biochemical assays (e.g., immunohistochemical staining and Western blotting), and histology. CFTR Cl^- secretion was measured by Ussing chamber following forskolin stimulation, but the formation of an intercellular lumina "blister" impeded the traditional measurement of CFTR function. Following culture conditions optimization, a CFTR knockout was generated through CRISPR/Cas9 lentivirus infection and confirmed via protein analysis. In parallel, healthy wild-type (WT) cells were compared to cells where CFTR was pharmacologically inhibited (i.e., CF-like cells) and showed differences in mucin concentrations. Our data suggests these mucin-producing cell lines can function as relevant *in vitro* models to study the CF gut mucus phenotype. Investigating pure mucus in an environment devoid of inflammatory cells and/or fecal matter can help focus on mucins' abnormal properties and reveal novel pharmaceutical targets. A treatment targeting mucins or reversing the abnormal mucus phenotype would be mutation agnostic (i.e., independent of genotype) and therefore would have the potential to slow the progression of the disease and benefit all patients with CF.

Acknowledgements

I would like to thank Dr. Camille Ehre and all of the Ehre Lab for their support, encouragement, and helpful critiques throughout the duration of this project. I would also like to thank Dr. Amy Maddox and the UNC Chapel Hill Biology Department for the guidance on writing and presenting the findings. And finally, I would like to thank my friends and colleagues who helped during this time.

Introduction

Cystic Fibrosis (CF) is a chronic life-threatening disease generally caused by a mutation in the cystic fibrosis transmembrane conductance regulator (CFTR) gene that decreases the ability of cells to effectively secrete chloride anions.[1] Subsequent water hyperabsorption in response to the ionic influx leads to an external buildup up of high-molecular-weight glycoproteins (mucins or MUCs) with decreased viscoelasticity unable to be cleared.[2] Mucins are critical macromolecules responsible for the viscoelastic properties of mucus and can accumulate quickly; the worst effects of which are seen in the lungs and intestinal tract.[3] This mucus buildup restricts organ function by obstructing the airway ducts and digestive tract, making it difficult to pass air and absorb nutrients necessary for growth and development.[1]

Recently, Trikafta, a triple combination therapy of CFTR modulators has made headlines for being approved for patients carrying a copy of the most common mutation (ΔF508) and can potentially treat 80 % of CF cases.[4] However, a prominent issue remains for patients who do not qualify for modulator therapy (e.g., rare mutations or nonsense mutations). A general cure for the disease has yet to be fully investigated, but a gene independent treatment would be ideal to potentially benefit the entire CF patient community.

While both airway disease progression and respiratory complications have proven to be the most life-threatening concern for the disease and our previous work enlightened the role played by CFTR on airway mucins, investigating the effects of CFTR function on intestinal mucus may provide insight into the shared mucus properties and reveal novel mucin-based targets. The traditional mouse model used to study CF has posed problems in studying intestinal mucus because it often presents an increased bacterial burden with inflammation and obstruction.[5] *In vivo* models are therefore not preferred as these additional phenotypic effects make it more difficult to study

pure mucus. An *in vitro* model instead provides more consistency allowing for reproducibility. To further investigate mucus properties and the effects of CFTR malfunction, we aim in this study to determine the best conditions for developing and studying a cell line that models the intestinal epithelium.

HT29 is a human colon adenocarcinoma cell line composed of enterocytes and mucus-secreting goblet cells with the potential to accurately model CF due to high mucus production and expression of functioning CFTR.[6&7] HT29 cells are semi-polarized to model the distinction in the human intestines of apical and basal sides. Cancer cells are generally unpolarized and stack on top of each other, but it is possible to induce polarization in HT29 to form a monolayer.[8] The HT29-MTX-E12 line was differentiated with methotrexate to further stimulate goblet cell metaplasia and better mimic colonic crypts.[9] This line should be ideal to study the impact of CFTR function on mucin production and organization because of these factors.[10]

It is important to ensure this differentiated line is as polarized as possible, so it pumps chloride and secretes mucins towards the apical lumen. Because HT29 is a cancer cell line, it tends to form multilayers rather than a single monolayer (Figure 1A). A balance must be established of an ordered epithelium that still possesses the features of colonic crypts. Since the HT29 line is initially only semi-polarized, it can form intercellular lumina (ITCL) which trap mucus and separate the cells (Figure 1B). Some cells secrete their wastes and products in towards what should be the basal side or towards other cells because they have not fully differentiated and/or polarized.[8] These ITCL make it difficult to accurately collect entrapped mucus as it is not open to the apical lumen, and they weaken tight junctions (i.e., lower resistance). *In vivo*, the intestinal epithelium must have strong tight junctions to sustain friction from intestinal transit while allowing nutrient absorption.[11]

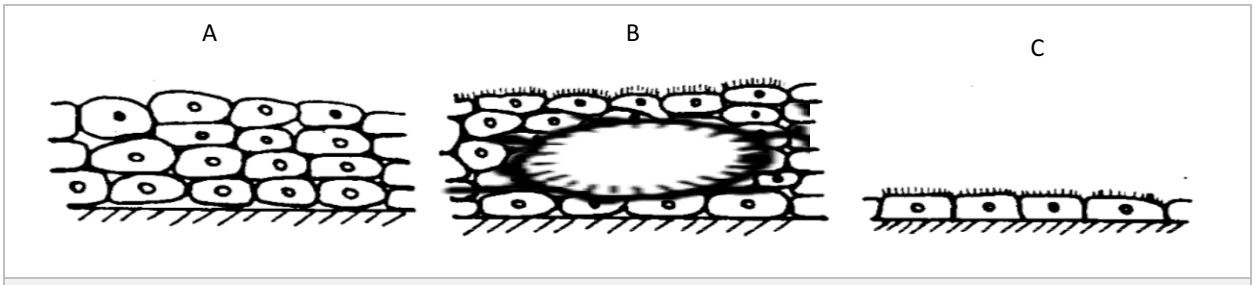

Figure 1. HT29 Polarization Influenced by Media Conditions.
A) Weakly polarized cell line. B) Semi-polarized cells with the presence of an ITCL. C) Polarized monolayer of cells. Modified from Hekmati et al.[8]

For 2D-planar models, cell polarization and resistance depend on environmental factors, such as the quality of the media, gas concentration, pH, and maintaining a sterile environment. While gas concentration, pH, and sterile environment are mostly standardized for *in vitro* models, we spent time testing different media to optimize the polarization and resistance of HT29-MTX-E12 cells. While McCoy's 5A is a standard base media for much of mammalian cell culture, Dulbecco's Modified Eagle's Medium (DMEM) has come to be the most common HT29 cell culture media.[12] L-alanyl-L-Glutamine is incorporated into DMEM Glutamax as several studies have signified its prevalence in forming strong tight junctions and healthier cells because it does not degrade into ammonia as quickly as regular glutamine in most media.[13] The standard media encloses a low glucose concentration, but glucose supplements are offered. Our lab initially used high-glucose DMEM Glutamax based on a previous study indicating increased mucus production, but other studies suggested the absence of glucose lead to better gut epithelium differentiation.[14] Initial media testing in our lab also suggested better cell morphology when using lower glucose concentrations. RPMI 1640 is another cell culture media with intermediate glucose concentration that can induce strong polarity over time and can lead to a complete monolayer of HT29 cells.[8]

These media were compared to culture the HT29 cell line and to study the impacts on cell structure and organization as well as mucin production and CFTR function.

Even with the HT29-MTX-E12 differentiated cell line, mucus production is lower than *in vivo*.[15] Several studies point to treatment with DAPT (N-[N-(3,5-Difluorophenacetyl)-L-alanyl]-S-phenylglycine t-butyl ester) and mechanical stimulation as a method to increase goblet cell differentiation and promote the production of even more mucus.[7] Interestingly, a study showed that goblet cell metaplasia, known to be associated with increased mucin concentrations, was correlated with decreased CFTR expression.[3] For our project, the proper balance between CFTR expression/function and mucin secretion must be achieved to further study the effects of CFTR loss-of-function mutations on mucus production and mucus properties. For that, we tested different media to determine the best conditions for our study.

Different media recipes as well as treatment with and without DAPT and mechanical stimulation were investigated with a goal to obtain a well-differentiated cell layer mimicking the gut epithelium and to establish the best model to study mucus alterations in response to CFTR loss and gain of function with regards to the cystic fibrosis gut disease.

In *in vivo* conditions, the intestinal epithelium dominantly expresses MUC2 with traces of MUC5B and MUC5AC, the dominant mucin of the stomach that is also expressed in the lungs following pathogen infection.[16] MUC2 and MUC5AC as well as MUC5B, MUC6, and other less significant mucins are classified as gel-forming mucins. They are stored in secretory granules that are then released in response to agonists and expand in response to pH and ion level changes.[17] Once secreted, it is believed that the mucins polymerized in the endoplasmic reticulum and golgi can unfold to form net-like spreads over cells.[18] Studies have indicated that MUC2 forms dimers of trimers leading to hexagonal rings which may strongly impact the mucin network

ultrastructure.[19] However, MUC2 has been suggested to remain tethered to the cell membrane needing additional cleavage before total release.[20] Understanding these mucin properties is important to developing a mucin-based treatment centered on mitigating mucus abnormalities and could apply not only to CF but also to diseases with abnormal mucus properties like COPD and asthma for the lungs or IBD and Crohn's disease for the GI tract.

Recently, the Clustered Regularly Interspaced Short Palindromic Repeats (CRISPR)-associated (Cas) protein 9 system (CRISPR/Cas9) has become an increasingly popular tool to assist with DNA editing. This combination introduces double-strand breaks at precise sites determined by programmable sequence-specific guide RNAs (sgRNAs).[21] While it has proven value to clinical gene therapy studies for cancer and other diseases, it can also be used *in vitro* to modify cell lines. The non-homologous end joining (NHEJ) repair path of the double strand break is especially useful with CRISPR/Cas9 as it allows for efficient insertions and deletions, creating early stop mutations to fully knock out the expression of a specific gene. Compared to homologous-directed-repair (HDR), common for reverse back point mutation, NHEJ has a higher probability of occurring with less random chance.[22] Increasing our probability of gene editing is especially important for the HT29 cell lines as it is triploid, and therefore, requires mutations across all three chromosomes to initiate a CFTR knockout.[23] The CRISPR/Cas9 system produces stable mutations that persist across multiple passages since the mutation is fully incorporated into the genome of successfully manipulated cells.[24] We used the CRISPR/Cas9 method to generate a CFTR-KO HT29 cell line, and in parallel, we mimicked a CF-like phenotype by using bumetanide/dimethylamiloride (DMA) on WT HT29 cells to temporarily block chloride and bicarbonate secretion.[25]

The effects of CFTR function on mucin production in the gut remain poorly understood at this time. Most of the work has focused almost exclusively on lung cells and shown that *in vitro* CF airway models produce increased gel-forming mucin concentrations when compared to the WT controls. Our study provides a reliable *in vitro* gut model to explore the effects of CFTR function and loss-of-function on intestinal mucins. Additionally, our study identifies MUC2 as a permanently crosslinked mucin that remains tethered to cells in greater amounts than other secreted mucins. Pharmacological CFTR knockdown resulted in an increase in MUC5B but almost no change in MUC5AC concentration. The CFTR-knockout cell line, successfully generated by CRISPR, could further enlighten our findings. An improved understanding of CF mucin effects has the potential to be the key in developing genotype-independent treatments that may prevent disease progression and benefit all patients.

Experimental Methods

Cell Culture of HT29-MTX-E12 Cell line

HT29-MTX-E12 cells (Sigma-Aldrich) were grown on a T75 cm^2 culture-treated flask with 10 mL of media. They were incubated at 37°C, 5% CO_2 with media changed every 2 or 3 days. Once 90% confluent, the cells were rinsed with 1X PBS (Phosphate Buffered Saline) then detached with 0.25% EDTA-Trypsin. Cells were seeded in new flasks at a density of 5.0 $x10^5$ cells. Media was prepared by adding 10% Fetal Bovine Serum (FBS), 1% Non-Essential Amino Acids (NEAA) and 1% Penicillin Streptomycin to DMEM Glutamax Low Glucose (1 g/L glucose, Low) base medium (ThermoFisher Scientific). For experimental testing, HT29 cells were seeded into six 12-well 12mm diameter transwell tissue-culture treated plates at a density of $2.2x10^5$ cells/cm^2. Media were placed basolaterally (1.5 mL) and apically (200 μL) until cells

reached confluence. Upon confluence, apical media was reduced to 100 μL to obtain semi-wet conditions. Basolateral and apical media were removed and replaced every 2-3 days.

Characterization of HT29-MTX-E12 Cell line

Media Name	Glucose Concentration
DMEM Glutamax High Glucose (High)	4.5 g/L
DMEM Glutamax Low Glucose (Low)	1.0 g/L
RPMI 1640 (RPMI)	2.0 g/L

Table 1. Base Media Glucose Levels

Different media conditions were prepared by adding 10% FBS, 1% NEAA, and 1% Penicillin Streptomycin to the base media (Table 1). The full recipes for the base media can be found in the appendix (Table A1). For comparison purposes, the same passage of cells were plated and grown in parallel with High, Low or RPMI media. Once confluent, half of the cultures for each media were treated with 10 μM of DAPT N-[N-(3,5-Difluorophenacetyl)-L-alanyl]-S-phenylglycine t-butyl ester) basolaterally for 4 days and placed on a rocker in the incubator to stimulate crypt differentiation.[7]

At 2 days, 9 days, 16 days, and 23 days post-confluency, transepithelial electrical resistance (TEER) was measured with a World Precision Instruments Evom2 Epithelial Voltohmmeter. Different inserts were fixed for histological comparison or apical surfaces were washed for further analysis.

Once cells reached maturity (28 days post-confluency), cell washings were collected and analyzed via dot blot for mucin production. Briefly, cell washings were applied via aspiration onto a nitrocellulose membrane. The membrane was washed and co-probed with a primary rabbit

polyclonal anti-MUC2 (H300) antibody and a mouse monoclonal anti-MUC5AC (45M1) antibody and revealed with fluorescently labeled secondary anti-rabbit (green) and anti-mouse (red) antibodies. Signal was captured using a LI-COR infrared imaging system and quantified using the Odyssey LI-COR software.

CRISPR/Cas9 Plasmid Preparation and Lentivirus Production

Once HT29-MTX-E12 media and culture conditions were optimized, we proceeded to use this cell line to investigate the mucin response to CFTR malfunction by knocking out CFTR in the cell line. This gene editing approach was conducted using the CRISPR/Cas9 non-homologous end-joining method and encapsidation of the molecular tools (e.g., plasmids) into lentiviruses. To ensure an accurate retroviral target, two plasmids were obtained from abm Inc. (Figure 2). One plasmid carried the target sgRNA and Neomycin resistance (pLenti-U6-sgRNA-PGK-Neo), while the other plasmid carried the Cas9 and Puromycin resistance gene (pLenti-EF1a -Cas9-2A-Puro). For control, a plasmid similar to the first plasmid described above but containing a scrambled sgRNA was used to infect the cells. Amplifications of plasmids were achieved previously using the "α-Select Bronze Efficiency Chemically Competent Cells" kit (Bioline) via transformation and expansion. Plasmids were then purified using a QIAfilter maxi kit (QIAGEN) to extract DNA and then send to sequencing.

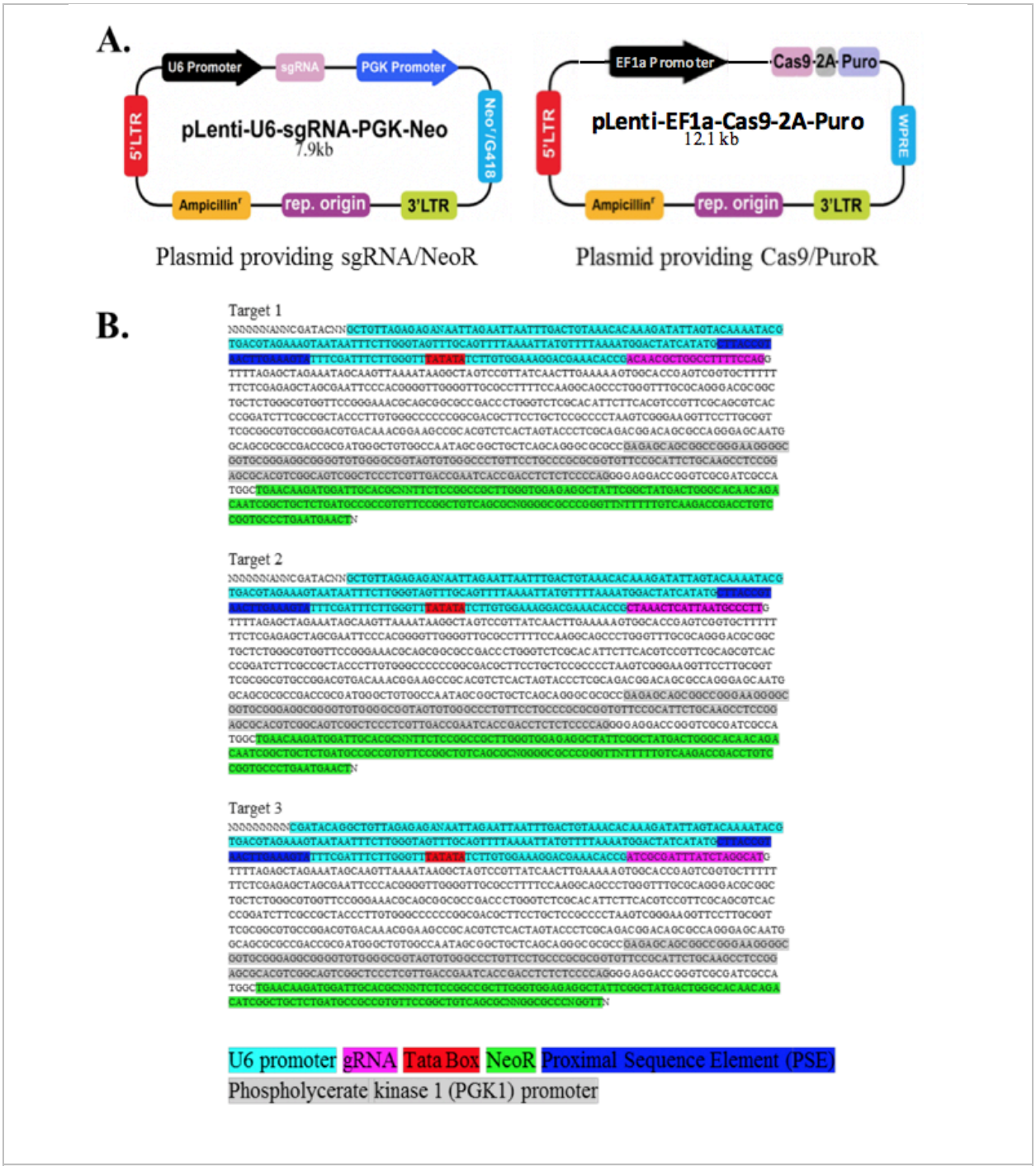

Figure 2. Plasmids Construction and Sequencing of CRISPR Target.
The plasmids containing guide RNA and Neomycin resistance were used to direct CRISPR insertion with addition of Cas9 with Puromycin resistance (A). Target 1 was selected initially with Targets 2 and 3 made as backups (B).

Once plasmid purification and sequencing were suitable, lentiviruses were prepared by mixing 1.75 mL of OptiMEM media with 7.5 mg of psVG packaging plasmid and 12 mg of

psPAX2 packaging plasmid. Additionally, 15 mg of purified plasmids (target or scrambled) was added and let mix for 5 minutes. A second mix was prepared with 3.5 mL of OptiMEM media and 70 mL of X-tremeGENE reagent (Millipore Sigma). After incubation for 5 minutes at room temperature, 1.75 mL of the mix containing the X-tremeGENE reagent was added to each of the two plasmid mixes. These two solutions, called "CFTR Target 1" and "CFTR Scrambled Control" plasmid mixes, were then incubated at room temperature for 20 minutes.

HEK cells were grown in DMEM base media with 10% FBS and 1% Penicillin Streptomycin until 80% confluent in a 15 cm culture treated plate. The two plasmid mixes were then added to the HEK cells separately and gently rocked to ensure even spread. Cells were returned to incubation at 37°C, 5% CO_2 for 6 hours. After the 6 hours, media was removed and cells were washed once with 1x PBS. After washing, 30 mL of DMEM supplemented with 10% FBS, 1% BSA, and 10 mM HEPES were added to the cells. They were then returned to incubation for 60 hrs. At this time, virus titer levels were tested using a Takara test kit and the lentivirus product was collected.

Lentivirus Transfection to Generate a HT29-MTX-E12-CFTR-KO Cell Line

Before transfection, HT29 cells were seeded at a density of 5.0 $x10^4$ cells/well in a 6-well tissue culture treated plate. After 3 days, the cells were at 30% confluence and lentivirus infection was started. $1x10^6$ Infectious Units of the Cas9 lentiviruses were added to four wells along with 3 μL of Polybrene. Two of these wells were mixed with $1x10^6$ Infectious Units of the CFTR Target 1 lentivirus, and two different wells received $1x10^6$ Infectious Units of the CFTR Scrambled Control lentivirus. The remaining two wells were kept as non-infected controls (WT). After 48 hours, selection was started with 1 mg/mL of Geneticin and 2 mg/mL of Puromycin in all wells except one of the WT controls to monitor cell viability. Antibiotic treatment was kept for 2 weeks

and cells were passaged as they neared confluence. To ensure successful gene editing, CFTR gene and protein expression were tested via DNA sequencing and SDS- PAGE Western blotting, respectively. Ussing Chamber analysis was performed by Nancy Quinney of the UNC Gentzsch Lab. Changes in transepithelial voltage were measured following specific ion channel inhibitions (e.g., amiloride for ENaC and inhibitor 172 for CFTR) and gating (e.g., forskolin for CFTR), reflecting the accuracy of the model to mimic the intestinal epithelium.

Pharmacological Inhibition of CFTR

In parallel, HT29 WT cells were treated with pharmacological agents (bumetanide and 5-(N,N-dimethyl)-amiloride or DMA) to induce abnormal ionic fluxes and mimic CF conditions.[25] HT29 WT cells were seeded in transwells in a 6-well plate using Teflon spacers at a density of 2.0 x 10^4 cells/cm^2. After 28 days of culture, cell blisters or intercellular lumina (ITCL) (Figure 1B) were carefully removed, and the cells were allowed to regain tight junctions for 5 days. Inserts were treated apically with 10 mM Bumetanide and 100 mM DMA, while other inserts were used as WT controls, receiving 1x DMSO. Treatment occurred once a day for 3 days. Apical media secretions were then collected and run in a Western blot to detect MUC2, MUC5B, and MUC5AC secretion. Change in signal intensity was quantified using a t test in GraphPad Prism 7.

Histology

For all conditions, cells were fixed with 10% NBF at 1, 2, and 3 weeks post-confluence. Fixed cell inserts were sent to be processed and sectioned by the UNC Animal Histopathology Core. Sections were left unstained for immunohistochemistry or stained with Hematoxylin/Eosin (H&E) and Alcian Blue/Periodic Acid-Schiff (AB-PAS). Immunohistochemical staining was

performed with primary rabbit polyclonal anti-MUC2 (H300) and mouse monoclonal anti-MUC5AC (45M1) fluorescent antibodies.

Results

HT29 MTX-E12 Characterization

To determine optimal culture conditions, we tested six media conditions (DMEM high and low glucose and RPMI; all three media tested with and without DAPT and mechanical stimulation). To examine cell morphology, cells were fixed and processed via histology to monitor the formation of a columnar monolayer and mucus production over time. Observation of the histological sections stained via H&E under a light microscope revealed the presence of large ITCL blisters for all media conditions tested. DMEM high glucose conditions appeared the least uniform, with uneven cell surfaces, while DMEM low glucose and RPMI conditions provided smoother cell layers with the formation of a semi-polarized dome of cells at the center of the inserts. At week 3 post confluence with DMEM low glucose, some of the domes started to break apart or peel off, suggesting further differentiation and increased polarization.

DAPT treatment increased goblet cell differentiation and mucus production, but the 2D cell layers lost their compact configuration. Instead of forming a semi-crypt morphology, the cell layer appeared less polarized with cells stacked on top of each other, resulting in an aberrant morphology (Figure 3). DMEM high glucose conditions also resulted in generally unpolarized cells, causing the mucus to spread throughout the cell layers. Cells grown in DMEM low glucose were semi-polarized with the formation of distinct ITCL. Prior to week 4 post confluence, DMEM low glucose allowed the formation of a cell monolayer but entrapped mucus in the ITCL with the blister of cells on top.

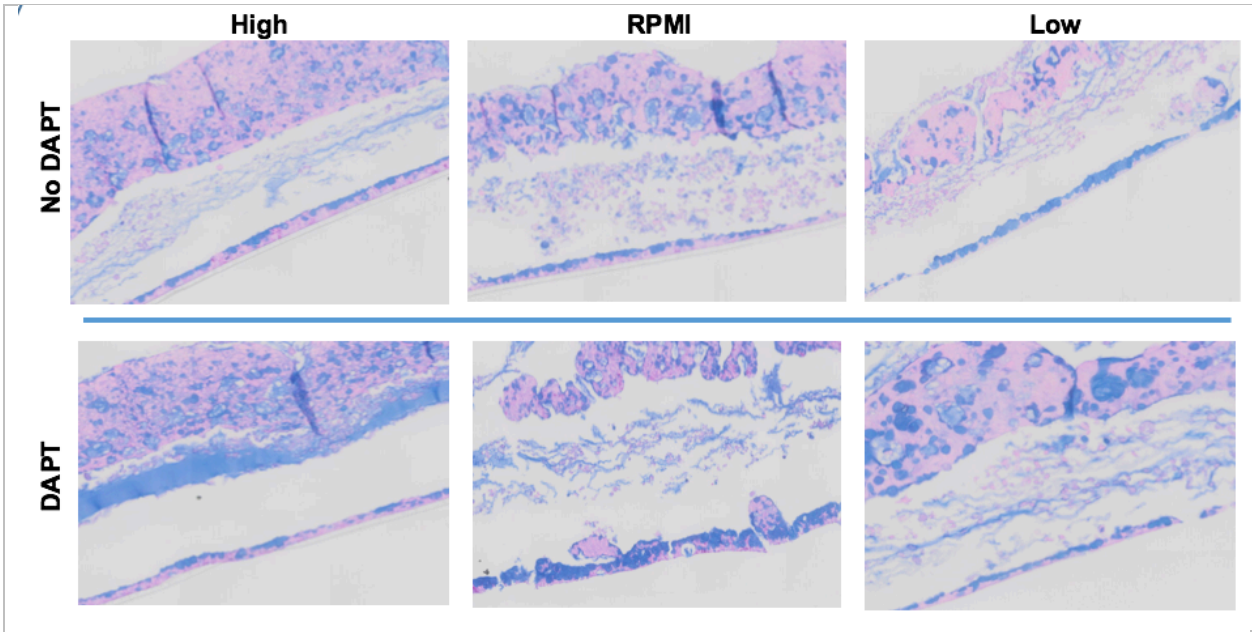

Figure 3. HT29 Differentiated with Different Culture Conditions.
Slides of WT HT29-MTX-E12 cells were fixed and stained with AB-PAS at 3 weeks post-confluence. High glucose DMEM Glutamax (High), RPMI 1640 (RPMI), and low glucose DMEM Glutamax (Low) media were tested resulting in differential cell columnar and blister growth. The addition of DAPT to is seen across the bottom row.

Post differentiation, the cells grown in DMEM high glucose with and without DAPT showed detachment from their membrane and aberrant growth. In contrast, cells grown in DMEM low glucose in the absence of DAPT formed a semi-polarized columnar monolayer.

Conditions using DMEM low glucose resulted in the greatest resistance while the DMEM high glucose conditions generally had the lowest TEER readings when measured with a WPI Evom2 (Figure 4A). This shows that the cells grown in DMEM low glucose formed tight junctions quicker and retained a stronger seal across the membrane. The inserts reached maximum resistance around one to two weeks, which correlated with peak blister seal. The higher the glucose concentration, the lower the resistance; cells grown in RPMI had intermediate resistance readings but were comparable to that of high glucose conditions. The relationship between DAPT treatment and resistance was more variable and remains unclear. A follow-up assessment that measured

resistance post differentiation and blister removal comparing DMEM low glucose with RPMI showed that cells grown in DMEM low glucose media recovered quicker and retained higher resistance (Figure 4B).

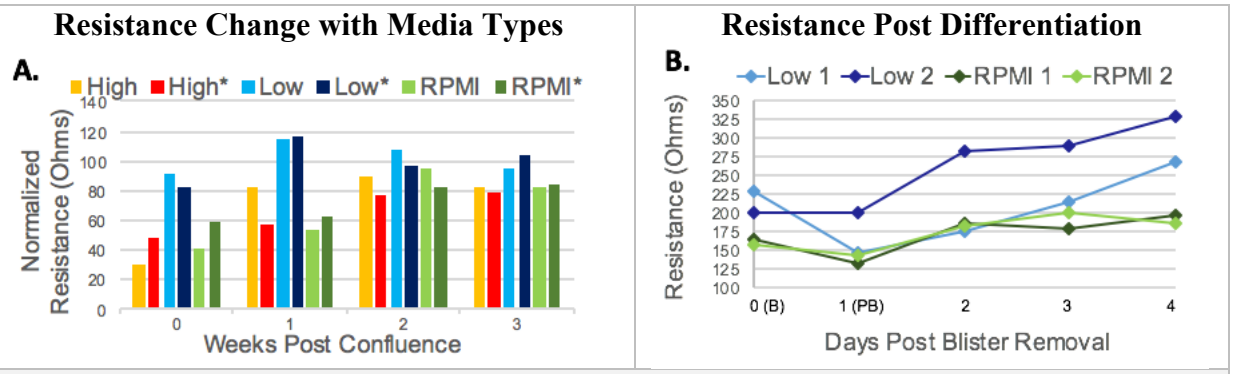

Figure 4. Resistance Change with Differentiation in Media Conditions.

A) TEER measured by WPI EVOM2 revealed changes over a 4-week period for all media conditions tested to growing HT29-MTX-E12 cells. *Asterisks indicate treatment with DAPT and mechanical stimulation.

B) TEER measurement post removal of the ITCL blister for cells grown in DMEM low glucose or RPMI media (1 and 2 reflect two different inserts of the same condition).

To quantify relative mucin production, we used dot blotting on apical cell washings over time. Each of the media conditions produced a relatively similar concentration of MUC5AC (Figure 5). Of all the conditions, DMEM low glucose initially showed the highest production of MUC5AC, but after roughly two weeks, this condition showed the lowest levels of MU5AC. DMEM high glucose produced the the most consistent and sustained MUC5AC production and an intermediate amount of MUC2. While pipetting, cells grown under DMEM high glucose appeared to have the most viscous mucus, but cells grown under low glucose ended up producing more MUC2, suggesting that MUC5AC possesses higher viscoelastic properties than MUC2. DAPT treatment slightly stimulated MUC2 production, but its effect on MUC5AC production is unclear. Overall, DMEM low glucose without DAPT provides the best results with a high concentration of MUC2 and an intermediate level of MUC5AC.

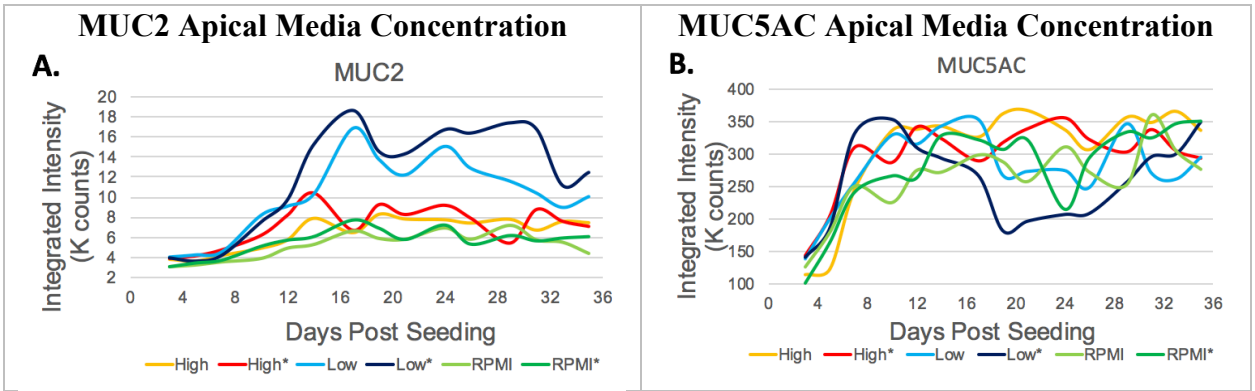

Figure 5. Mucin Production under the Different Media Conditions.

A) Dot blot assay shows the relative change in MUC2 production for each condition over several days (0-36) of culture.

B) Relative signal intensity by dot blot for the mucin MUC5AC for each condition over several days (0-36) of culture.

*Asterisks indicate treatment with DAPT and mechanical stimulation.

The results showed that over time, wildtype HT29 cells produced an increasing amount of both MUC5AC and MUC2. While MUC5AC was clearly present in apical washings, MUC2 appeared to be at lower concentrations. However, cell lysates analyzed by Western blotting revealed that both mucins, especially MUC2, were at higher levels intracellularly or attached to the cell surfaces (Figure 6B). Immunohistochemistry revealed that MUC2 was located inside mucin granules that were clustered rather than coating the cell surfaces (Figure 6A). Additionally, MUC2 and MUC5AC signals did not co-localize, which could suggest different machineries or signaling pathways for secretion.

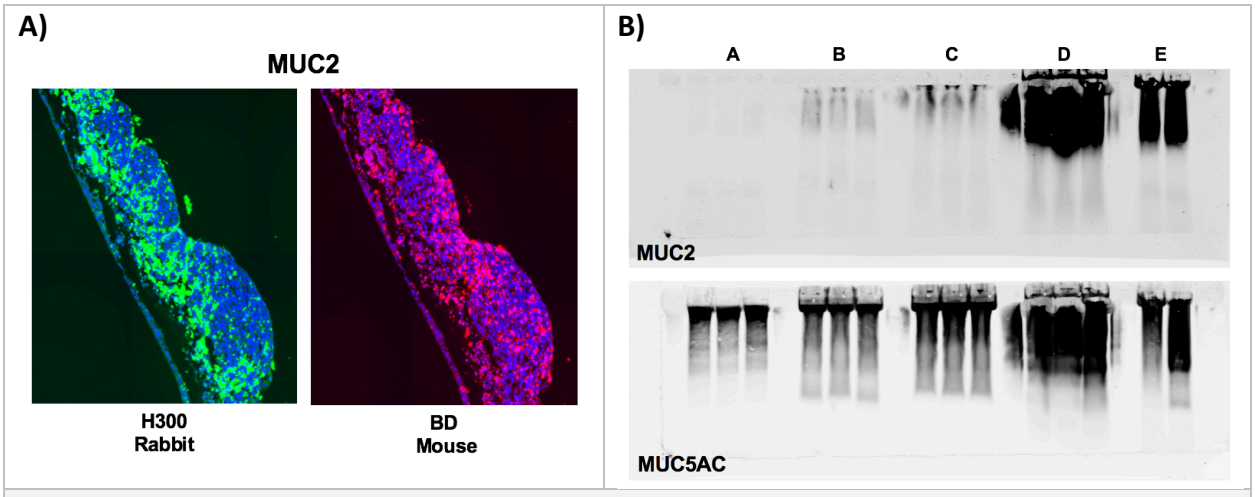

Figure 6. Immunohistochemistry and Western blotting to detect Mucin Localization and Production in Cultures.

A) HT29 cultures were fixed, processed for histology, and sections were stained with a rabbit anti-MUC2 (H300) (green) or a mouse anti-MUC2 (BD) (red) antibody.

B) Western blot of HT29 washings, cell and blister lysates, showing signal for MUC2 (top blot) and MUC5AC (bottom blot) production. 3 cell washings were run for week 1 (A), week 5 (B), and week 3 (C). 3 cell lysates were run for week 3 (D) and 2 blister lysates for week 4 (E).

Ussing chamber results from a preliminary study were inconclusive with the HT29 cell line, but the same cells cultured in DMEM low glucose media without DAPT maintained CFTR function (Figure A2). The absence of distinct peaks suggested issues regarding CFTR expression and pharmacological inhibition for all the tested conditions.

CRISPR/Cas9 gene editing to create a HT29 MTX-E12 CFTR-KO cell line

In order to mimic a CF environment, we generated a CFTR knockout line of HT29-MTX-E12, using the CRISPR/Cas9 NHEJ approach. This method necessitated we acquired and purified plasmids with the target sequence and antibiotic resistance to encapsulate into lentiviruses. These lentiviruses were used to transfect WT cells, which were then treated with antibiotics to eliminate cells where transfection was unsuccessful. Antibiotic selection resulted in the death of all selected wild type cells while those transfected with either CFTR Scrambled Control or CFTR Target 1 survived. Unselected wildtype cells continued to survive and reach confluence quickly identifying

the antibiotic selection as the differing factor (Figure 7A). The CFTR Target 1 cells were then sequenced and analyzed for CFTR protein. Sequencing showed almost no presence of unaltered CFTR DNA, and SDS-PAGE showed a lack of a band of CFTR protein in the knockout identifying a successful knockout (Figure 7B).

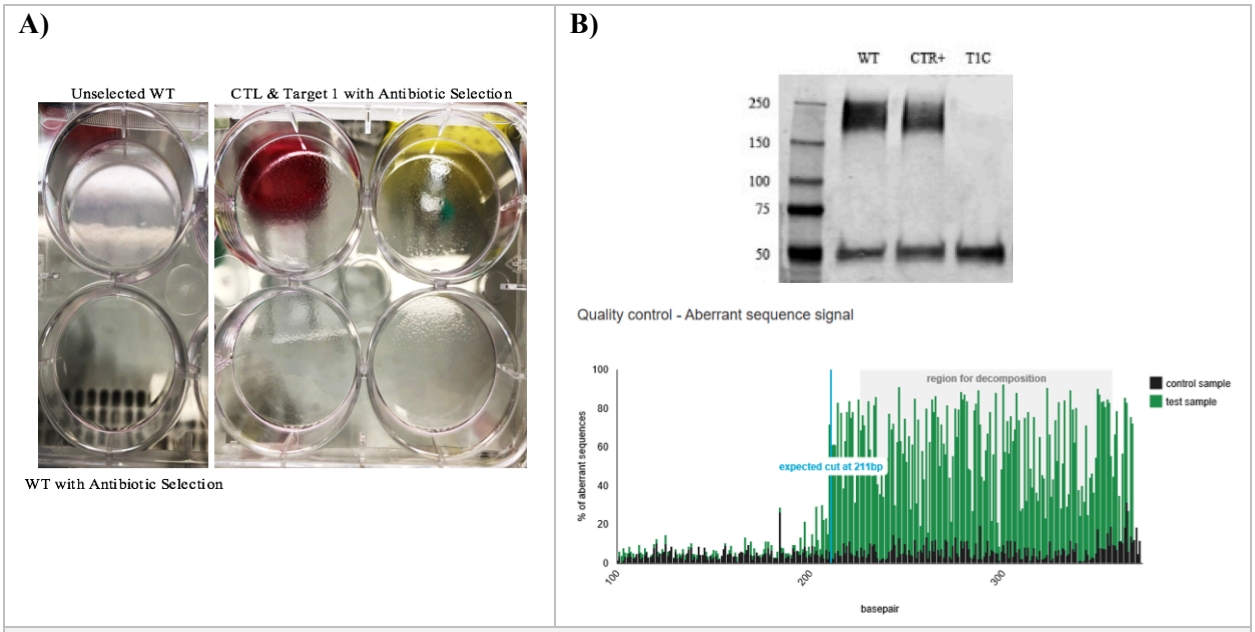

Figure 7. Virus Transfection and Knockout Generation.

A) The left column of wells tested the selection of the Geneticin and Puromycin antibiotics. The center column of wells shows Control transfection cell growth under selection, and the right column shows Target 1 transfected cell growth with selection.

B) SDS-PAGE of cell lysates and DNA sequencing show CFTR protein level (band just below 250) and aberrant CTFR sequence respectively.

While generating the CFTR KO cell line, wildtype cells were used to mimic disease state through pharmacological inhibition of CFTR. This inhibition provided a temporary model to investigate short term mucin changes. Pharmacological inhibition resulted in an increase in mucins quantified by Western blot (Figure 8). While MUC5AC did not significantly increase in the chemically knocked down cells, MUC5B did significantly increase. MUC2 appears to have a significant decrease in the CFTR knockdown (Figure 8).

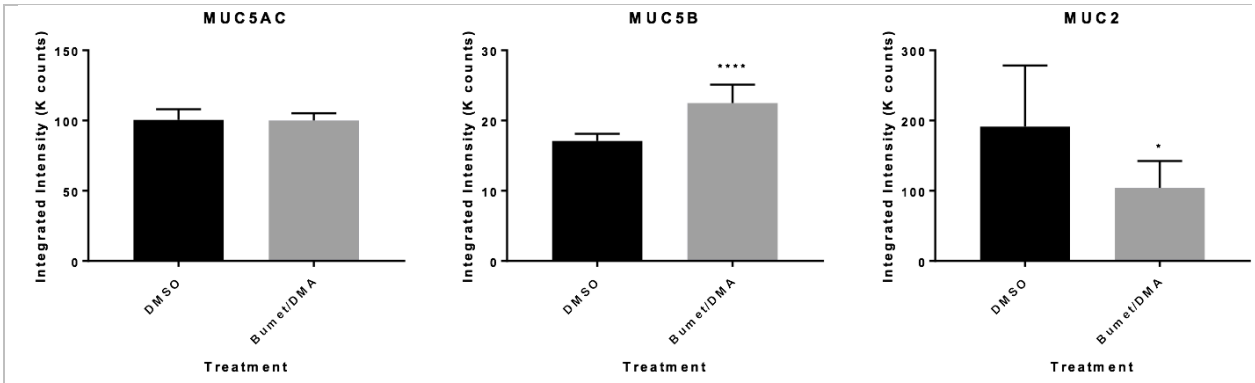

Figure 8. Pharmacological Inhibition of CFTR Affects Mucin Concentrations.
GraphPad Prism7 t-test analysis and boxplots quantify mucin concentrations of HT29 apical media collections. DMSO acts as a control while Bumetanide/DMA represents cells with CFTR pharmacological inhibition.

Discussion

Our goal was to better characterize intestinal mucus and to generate a model that was optimized to study pure mucins *in vitro*. Current literature mainly focuses on airway mucus response to CFTR malfunction, while the systemic problem of aberrant mucus phenotype in several organs in CF suggests that all gel-forming mucins develop aberrant properties in CF. Studies not related to CF have suggested that intestinal cultures treated with DAPT, mechanical stimulation, and high levels of glucose may generate a model more similar to *in vivo* conditions.[7&8] With this work, we demonstrated that HT29-MTX-E12 can fill the void and be appropriately used as an intestinal *in vitro* model. Cultures in low glucose media without the presence of DAPT and mechanical stimulation resulted in optimal mucus production and histology, and genetic manipulation to generate a CFTR knockout HT29 cell line mimicking the CF environment was successful.

DMEM low glucose media resulted in the tightest polarized monolayer of cells. Additionally, this media condition resulted in the highest membrane resistance, and the cells were able to recover after ITCL blister removal. RPMI resulted in intermediate TEER values, which may be due in part to the presence of L-Glutamine affecting tight junctions. An RPMI Glutamax

media could have resulted in slightly higher resistance due to less ammonia generation and cell damage, but this does not seem to be as important of a factor as glucose concentration. DMEM low glucose media produced the highest concentration of MUC2 and an average MUC5AC concentration. While DAPT increased mucin concentrations, it resulted in abnormal histology due to cell metaplasia. Antibody staining showed that MUC2 is in much higher concentration intracellularly or tethered to the cells than detected in the lumen in the secreted form. The CFTR CRISPR/Cas9 transfected cells survived through selection and showed an absence of functional CFTR while the WT, untransfected cells did not survive antibiotic selection as expected. Pharmacological inhibition of CFTR resulted in increases of some mucins (MUC2 & MUC5B), but MUC5AC remained relatively unchanged.

Overall, low glucose DMEM Glutamax media without DAPT or mechanical stimulation provided the best results for cell growth and mucin production. It was the only media in which cells fully differentiated to a monolayer without dying or losing polarity. The resulting high MUC2 levels in low glucose media are ideal as this is the major mucin of the gut and crucial for studying mucin properties. The presence of an intermediate, average concentration of MUC5AC is also important as it has comparative levels with lung mucus. The higher resistance seen in low glucose media additionally suggests its superiority as a model with stronger tight junctions necessary for investigating ion transport.

Our findings diverge from recent literature as DAPT and mechanical stimulation resulted in poor growth and less stability. Our suspicions were supported as well that lower glucose slows growth and results in a preferable polarized monolayer. Ussing results were inconclusive on how these conditions affected CFTR. This was likely due to the cells' semi-polarized nature with ITCL blisters interrupting directional CFTR ion transfer.

Investigation of mucin localization supported the idea that MUC2 may remain either within granules or stay tethered to cell membranes. The high concentration and visualization inside cells reinforces this idea suggesting additional steps may be taken naturally when releasing the mucin. While MUC2 is classified as a secreted gel forming mucin, our data shows that it may take a different path to secretion resulting in difficulty measuring mucin level if it remains attached. This finding could potentially impact past results if the level of MUC2 present does not match what was collected.

The CRISPR/Cas9 knockout was successful in interrupting the CFTR gene. This resulted in a cell line devoid of CFTR that can function as a CF model. Combined with other findings of histology, adequate mucus levels, and CFTR response in WT cells, the HT29 transfected cells provide a key model to further investigate direct mucus effects of CF. The pharmacological inhibition provides an alternate model in which CFTR is temporarily inactivated. This matched with previous studies of airway cells showing an increase in mucus, but interestingly MUC5AC concentration remained the same. Cystic Fibrosis may not affect MUC5AC unanimously across the body. MUC2 levels showed a decrease when quantified but this is likely due to either mucins unable to transfer through the agarose gel in the western blot due to their complex polymerization network or due to remaining tethered to cells.

Successful optimization and transfection of the HT29 cell line as a gut model allows for future directions in developing a mucin-based, genotype independent treatment for CF and other mucus based diseases. While traditional Ussing chamber exploration has been inconsistent with HT29 cells, FLIPR, a method of fluorescently labeling functioning CFTR, could provide more clarity. Our next steps will be to introduce specific mutations into the CFTR knockout line to investigate if these mutations share common impacts on both mucus and CFTR.

References

1. About Cystic Fibrosis. *Cystic Fibrosis Foundation* 1–7 (2015). Available at: http://www.cfww.org/about/article/400/.
2. Gadsby, D., Vergani, P. & Csanády, L. The ABC protein turned chloride channel whose failure causes cystic fibrosis. *Nature* 440, 477–483 (2006).
3. Kreda, S. M., Davis, C. W. & Rose, M. C. CFTR, Mucins, and Mucus Obstruction in Cystic Fibrosis. *Cold Spring Harb. Perspecitives Med.* 2, 171–176 (2012).
4. Lopes-Pacheco, Miquéias. CFTR Modulators: The Changing Face of Cystic Fibrosis in the Era of Precision Medicine. *Frontiers in Pharmacology* 10 (2019).
5. van der Doef, H. P., Kokke, F. T., van der Ent, C. K., & Houwen, R. H. Intestinal obstruction syndromes in cystic fibrosis: meconium ileus, distal intestinal obstruction syndrome, and constipation. *Current Gastroenterology Reports*, 13(3), 265-270 (2011).
6. Baudouin-Legros, M. *et al.* Modulation of CFTR gene expression in HT-29 cells by extracellular hyperosmolarity. *Am.J.Physiol Cell Physiol.* 278, 0 (2000).
7. Navabi, N., McGuckin, M. A. & Lindén, S. K. Gastrointestinal Cell Lines Form Polarized Epithelia with an Adherent Mucus Layer when Cultured in Semi-Wet Interfaces with Mechanical Stimulation. *PLoS One* 8, (2013).
8. Hekmati, M., Ben-Shaul, Y. & Polak-Charcon, S. A morphological study of a human adenocarcinoma cell line (HT29) differentiating in culture. Similarities to intestinal embryonic development. *Cell Differ. Dev.* 31, 207–218 (1990).
9. Leteurtre, E. *et al.* Differential mucin expression in colon carcinoma HT-29 clones with variable resistance to 5-fluorouracil and methotrexate. *Biol. Cell* 96, 145–151 (2004).
10. Pelaseyed, T. *et al.* The mucus and mucins of the goblet cells and enterocytes provide the first defense line of the gastrointestinal tract and interact with the immune system. *Immunol. Rev.* 260, 8–20 (2014).
11. Groschwitz, K. R. & Hogan, S. P. Intestinal Barrier Function: Molcular Regeneration and Disease Pathogenesis. *J. Allergy Clin. Immunol.* 124, 3–20 (2009).
12. Yang, Z. & Xiong, H.-R. Culture Conditions and Types of Growth Media for Mammalian Cells. *Biomed. Tissue Cult.* 3–18 (2012).
13. ThermoFischer. GlutaMAX media Keep your cells healthier for longer. 1–3 (2017). Available at: https://www.thermofisher.com/se/en/home/life-science/cell-

culture/mammalian-cell-culture/media-supplements/glutamax-media.html.

14. Zweibaum, A. *et al.* Enterocytic differentiation of a subpopulation of the human colon tumor cell line HT-29 selected for growth in sugar-free medium and its inhibition by glucose. *J. Cell. Physiol.* 122, 21–29 (1985).
15. Lee, B. H. & Kim, Y. S. Differential Mucin Gene Expression Associated with Methotrexate Resistance of Human Colonic Adenocarcinoma Cell Line, HT29. *J. Korean Cancer Assoc.* 29, 977–983 (1997).
16. Kim, Y. S., & Ho, S. B. Intestinal goblet cells and mucins in health and disease: recent insights and progress. *Current Gastroenterology Reports*, *12*(5), 319-330 (2010).
17. Verdugo, P. Supramolecular dynamics of mucus. *Cold Spring Harbor Perspectives in Medicine*, *2*(11) (2012).
18. Sheehan, J. K., Kirkham, S., Howard, M., Woodman, P., Kutay, S., Brazeau, C., Buckley, J. & Thornton, D. J. Identification of molecular intermediates in the assembly pathway of the MUC5AC mucin. *Journal of Biological Chemistry*, *279*(15), 15698-15705 (2004).
19. Nilsson, H. E., Ambort, D., Bäckström, M., Thomsson, E., Koeck, P. J., Hansson, G. C., & Hebert, H. Intestinal MUC2 mucin supramolecular topology by packing and release resting on D3 domain assembly. *Journal of molecular biology*, *426*(14), 2567-2579 (2014).
20. Schütte, A., Ermund, A., Becker-Pauly, C., et al. Microbial-induced meprin β cleavage in MUC2 mucin and a functional CFTR channel are required to release anchored small intestinal mucus. *Proceedings of the National Academy of Sciences*, *111*(34), 12396-12401. (2014).
21. Firth, A. L., Menon, T., Parker, G. S., Qualls, S. J. et al. Functional gene correction for cystic fibrosis in lung epithelial cells generated from patient iPSCs. *Cell Reports*, *12*(9), 1385-1390 (2015).
22. Iliakis, G., H. Wang, A. R. Perrault, W. Boecker, B. Rosidi, F. Windhofer, W. Wu, J. Guan, G. Terzoudi, & G. Pantelias. Mechanisms of DNA double strand break repair and chromosome aberration formation. *Cytogenetic and genome research* 104(4) 14-20. (2004).

23. Chen, T. R., Drabkowski, D., Hay, R. J., Macy, M., & Peterson Jr, W. WiDr is a derivative of another colon adenocarcinoma cell line, HT-29. *Cancer Genetics and Cytogenetics*, *27*(1), 125-134 (1987).
24. Cox, D. B. T., Platt, R. J., & Zhang, F. Therapeutic genome editing: prospects and challenges. *Nature medicine*, *21*(2), 121 (2015).
25. Ballard, S. T., Evans, J. W., Drag, H. S., & Schuler, M. Pathophysiologic evaluation of the transgenic CFTR "gut-corrected" porcine model of cystic fibrosis. *American Journal of Physiology-Lung Cellular and Molecular Physiology*, *311*(4), 779-787 (2016).

Appendix

Table A1. Base Medium Full Formularies.

Media	High Glucose DMEM Glutamax	Low Glucose DMEM Glutamax	RPMI 1640
Components	**mM**	**mM**	**mM**
Amino Acids			
Glycine	0.4	0.4	0.13333334
L-Alanyl-Glutamine	3.9723501	3.9723501	
L-Arginine			1.1494253
L-Arginine hydrochloride	0.39810428	0.39810428	
L-Asparagine			0.37878788
L-Aspartic acid			0.15037593
L-Cystine		0.15335463	
L-Cystine 2HCl	0.20127796		0.20766774
L-Glutamic Acid			0.13605443
L-Glutamine			2.0547945
L-Histidine			0.09677419
L-Histidine hydrochloride-H2O	0.2	0.2	
L-Hydroxyproline			0.15267175
L-Isoleucine	0.8015267	0.8015267	0.3816794
L-Leucine	0.8015267	0.8015267	0.3816794
L-Lysine hydrochloride	0.7978142	0.7978142	0.21857923
L-Methionine	0.20134228	0.20134228	0.10067114
L-Phenylalanine	0.4	0.4	0.09090909
L-Proline			0.17391305
L-Serine	0.4	0.4	0.2857143
L-Threonine	0.79831934	0.79831934	0.16806723
L-Tryptophan	0.078431375	0.078431375	0.024509804
L-Tyrosine		0.39779004	
L-Tyrosine disodium salt dihydrate	0.39846742		0.11111111
L-Valine	0.8034188	0.8034188	0.17094018
Vitamins			
Biotin			8.20E-04
Choline chloride	0.028571429	0.028571429	0.021428572
D-Calcium pantothenate	0.008385744	0.008385744	5.24E-04

Folic Acid	0.009070295	0.009070295	0.002267574
Niacinamide	0.032786883	0.032786883	0.008196721
Para-Aminobenzoic Acid			0.00729927
Pyridoxine hydrochloride	0.019417476	0.019417476	0.004854369
Riboflavin	0.00106383	0.00106383	5.32E-04
Thiamine hydrochloride	0.011869436	0.011869436	0.002967359
Vitamin B12			3.69E-06
i-Inositol	0.04	0.04	0.19444445
Inorganic Salts			
Calcium Chloride (CaCl2) (anhyd.)	1.8018018		
Calcium Chloride (CaCl2-2H2O)		1.7959183	
Calcium nitrate (Ca(NO3)2 4H2O)			0.42372882
Ferric Nitrate (Fe(NO3)3"9H2O)	2.48E-04	2.48E-04	
Magnesium Sulfate (MgSO4) (anhyd.)	0.8139166		0.407
Magnesium Sulfate (MgSO4-7H2O)		0.8130081	
Potassium Chloride (KCl)	5.3333335	5.3333335	5.3333335
Sodium Bicarbonate (NaHCO3)	44.04762	44.04762	23.809525
Sodium Chloride (NaCl)	110.344826	110.344826	103.44827
Sodium Phosphate dibasic (Na2HPO4) anhydrous			5.633803
Sodium Phosphate monobasic (NaH2PO4-H2O)	0.9057971	0.90384614	
Other Components			
D-Glucose (Dextrose)	25	5.5555553	11.111111
Glutathione (reduced)			0.003257329
Phenol Red	0.039851222	0.039851222	0.013283741
Sodium Pyruvate	1	1	

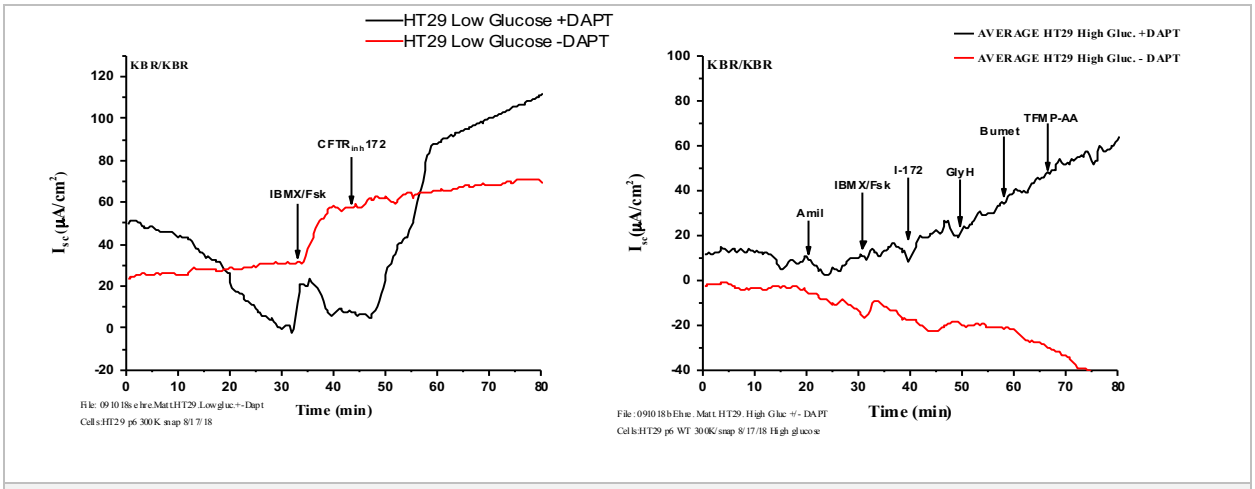

Figure A2. Ussing chamber current signifies CFTR function

HT29-MTX-E12 cells grown under DMEM low glucose conditions (left) and DMEM high glucose (right) show current changes in response to CFTR modulators in an Ussing chamber.